



A NEW CONTROLLER FOR SERIES ACTIVE POWER FILTER

YASEMIN ONAL

Dept. of Electrical and Electronic Engineering, Bilecik Seyh Edebali University

11210, Bilecik, Turkey & Mobile No: 0228 214 11 11

Email: yasemin.onal@bilecik.edu.tr

DOI: [10.33329/ijoer.76.26](https://doi.org/10.33329/ijoer.76.26)



YASEMIN ONAL

ABSTRACT

The nonlinear loads in power systems cause some undesirable situations such as current harmonic, voltage harmonic, voltage disturbance and voltage unbalance. To eliminate voltage harmonics and disturbances, the power electronic circuits based on serial active power filter (S-APF) is connected to power systems. In this study, synchronous reference frame (SRF) based a new controller using moving average filter (MAF) and space vector-PWM (SV-PWM) technique is proposed to the three-phase S-APF. In the proposed control algorithm, the MAF and SV-PWM technique are used to obtain the switching signals of active switches used in serial active filters. MAF to improve the transient response of the controller and SV-PWM technique to improve the performance of controller are used. Measurement values are taken from two different points of the power system and are used to calculate the reference load voltage values. In the algorithm, the number of measurements is reduced and the performance is improved by using source ab voltage and load abc voltage measurements. Simulation studies of the proposed controller for S-APF were tested using PSIM software and were compared with other control algorithms used in the literature. According to the simulation results, it is seen that the proposed controller for three-phase S-APF is more successful in eliminating the harmonics in the load voltage than the conventional SRF-based controller.

Key words—Series active power filter, Power factor, Total harmonic distortion, Moving average filter, Space vector PWM, Simulation.

I. INTRODUCTION

This document is a template. An electronic copy can be downloaded from the conference website. For questions on paper guidelines, please contact the conference publications committee as indicated on the conference website. Information about final paper submission is available from the conference website.

Today, energy quality has become an important factor with the usage of advanced devices. The current and voltage harmonics occur in the power system with the increasing use of

nonlinear power electronics circuits. The voltage unbalance, voltage sags and swells, harmonics in current and voltage are some examples to the problems created by power quality. Harmonic current and voltage cause fault of capacitors, noisy operation of electric machines, increased iron and copper losses in used machines and overheating of electronic devices[1-2].

Passive and active power filters are used to elimination power quality problems such as harmonic current and voltage, power factors and reactive power in the literature. The circuit structure

of the passive power filter PPF is simple, low in cost. But PPF's have some disadvantages such as their large size, the limitations, drawbacks of their usage and constant compensation problem [3]. Due to these disadvantages, active power filters APF is used to increase the filter performance [4-5]. APF's have been developed by the operation of active switches at very high frequencies. APF allows to suppress the harmonics in voltage and current with high frequency, perform reactive power compensation, eliminate some unbalances in three-phase systems and reduce neutral line currents [6].

In the literature, advanced flexible AC transmission systems (FACTS) are used to increase performance in voltage regulation and to perform instantaneous active and reactive power control. In addition, there are also custom power devices (CPD) for power quality problems. APF [7], dynamics voltage rectifiers (DVR) [8], distribution static converter (STATCOM) [9] are used for reactive power compensation and voltage regulation. There are studies on unified power quality conditioner UPQC systems that produce a wide range of solutions for power quality problems [10,11]. The UPQC is an APF system obtained by using a serial active power filter S-APF and a parallel active power filter P-APF. The parallel active power filter is used to filtering to current harmonics, current unbalances, reactive power compensation and neutral current compensation [12]; the S-APF is used to filtering source voltage harmonics, voltage unbalances and voltage drop/swelling[13,14].

In the literature, there are many control algorithms in the frequency domain and time domain which are applied to S-APF systems successfully. The control algorithms used in the frequency domain are not widely used due to large calculations and time and delay in the calculation of the FFT. In the time domain control algorithms used for S-APF, the derivatives of voltage signal are calculated. Commonly-used time domain control algorithms are the instantaneous active and reactive power based algorithms [14-15], synchronous reference frame SRF based algorithms [16,17], But, SRF based control algorithms show superior performance compared to PQ based algorithms [18]. In the SRF-based control algorithms, the low pass

filter LPF or high pass filter HPF is generally used for obtaining the reference current signal and sinusoidal PWM or hysteresis PWM is used for obtaining switching signals [19–21].

In this study, SRF-based a new controller using moving average filter(MAF) and space vector PWM (SV-PWM) is proposed for three-phase S-APF system. MAF filter and SV-PWM technique are used to obtain the reference voltage signals used in S-APF to reduce THD and to increase PF. In the algorithm, the number of measurements is reduced and the performance is improved by using source voltage and load voltage measurements without using source and filter current, filter voltage and load current measurements. Simulation studies of the proposed control algorithm were tested using PSIM software and were compared with other control algorithms used in the literature.

MATERIALS

Space Vector Pulse Width Modulation

In the SV-PWM technique, the aim is achieved to reveal the sinusoidal output voltage with the lowest switching loss and the lowest total harmonic distortion. For this, the possible switching states of the IGBT switches in the S-APF are expressed by a switching vector and are used with different combinations of these vectors. The most suitable switching scheme is selected. In this technique, the comparison isn't made in the determination of switching signals. The on-off times of the IGBT's are determined digitally.

In a three-phase SV-PWM inverter operating in six-step mode, switching states are changed every sixth of a cycle. The four possible phase-to-neutral voltage levels are $\pm V_{dc}/3$ and $\pm 2V_{dc}/3$. The sequence of the six switching states is such that only one switch changes state at a time. This sequence produces three phase voltages, displaced 120 [22]. For symmetric three phase voltages, the resulting space-vector sweeps a continuous circular path in the imaginary-real reference frame. It rotates at the frequency of the source voltages. If, however, a three leg inverter supplies the voltage, there are only six angular positions the voltage space vector can take at any instance. The three-leg inverter results in possible

space-vector positions. The six nonzero vectors form a hexagon. These space vectors can be calculated by multiplying the voltage-to-ground at the inverter terminals $\pm V_{dc}/3$ determined by the switching state, and the angular displacement of the stator phase windings

SV-PWM is considered to be a preferable technique of PWM applications, as it improves harmonic performance, reduces THD and provides better basic output voltage. Fig.1 shows d-q space vector coordinates of SV-PWM.

The d-q values of the abc voltages are calculated using Eq. (1).

$$\begin{aligned} V_d &= V_{sa} - V_{sb} \cos 60 - V_{sc} \cos 60 \\ V_q &= V_{sb} \cos 30 - V_{sc} \cos 30 \end{aligned} \quad (1)$$

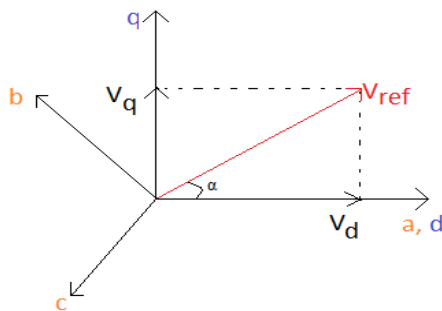


Fig. 1 Voltage dq coordinates

The magnitude $\overline{V_{ref}}$ and angle α of the rotating vector are calculated using Eq. (2).

$$\begin{aligned} |\overline{V_{ref}}| &= \sqrt{V_d^2 + V_q^2} \\ \alpha &= \tan^{-1} \left(\frac{V_q}{V_d} \right) = \omega_s t = 2\pi f t \end{aligned} \quad (2)$$

After this transformation, six active vectors and two zero vectors appear [23]. Using the Eq. (3), the time change between sectors 1 and 6 (S_1 - S_6) is determined ($n = 1, 2, \dots, 6$ and $0 \leq \alpha \leq 60^\circ$). Here T_m and T_{m+1} values are the application time of the voltages. T_0 is the application time of the zero voltage vector (V_0 or V_7) [24].

$$\begin{aligned} T_m &= T_s m \frac{\sqrt{3}}{2} \sin \left(\frac{n}{3} \pi - \alpha \right) \\ T_{m+1} &= T_s m \frac{\sqrt{3}}{2} \sin \left(\alpha - \frac{n-1}{3} \pi \right) \\ T_0 &= T_s - T_1 - T_2 \end{aligned} \quad (3)$$

The total of 6 space vectors are formed when the output voltages are studied for the period T and when the V_{ref} voltage vector is examined in the dq axis. These vectors are placed at 60° degree intervals in the standing axis tool. The switching states vary in each region. Fig. 2 shows the possible space-vectors. SV-PWM technique does not require carrier and reference wave forms such as sinusoidal-PWM technique.

Moving Average Filter MAF

The MAF is characterized by being an easy-to-implement filter capable of rejecting the multiple frequency components of the cut off frequency, which is defined as the inverse of the integration period or by the fundamental component period. Also MAF is used to improve dynamic filtering response. The discrete transfer function is calculated with (4) for modelling the MAF. n, denotes the number of sampling data used to derive average amounts[25].

$$H(z) = n^{-1} \left(1 + \frac{1}{z^1} + \frac{1}{z^2} + \dots + \frac{1}{z^{n-1}} \right) = \frac{1}{n} \frac{1-z^{-n}}{1-z^{-1}} \quad (4)$$

Fig. 3 shows the structure of the MAF. It is assumed that even harmonics are not present in the voltage or current. MAF filter is consists of the integration block, the transport delay block, the subtract block and the division block.

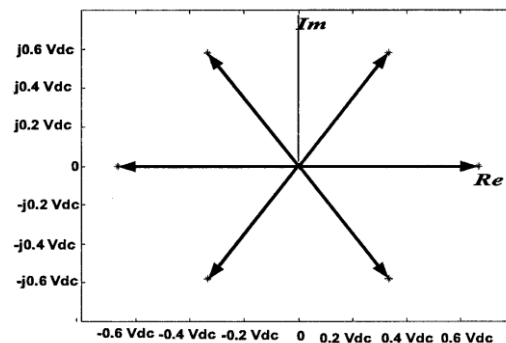


Fig. 2 Possible space-vectors



Fig. 3 MAF control block

The input voltage or current signal is delayed by the delay block. The transport delay block output is the current or voltage integral value delayed by 1/6 of the fundamental period. The integrator block output minus the transport delay block output represents the current or voltage integration over the interval $[t-T/6, t]$, where T is the fundamental period. The output of the subtract block is sent to the division block. Finally, the division block divides the integrated current or voltage by the integration interval, that is, $T/6$. Therefore, the outputs obtained from the products block are the moving average of i_d and v_d calculated over 1/6 of the fundamental period. Thereby, the output of the MAF is the moving average of the voltage signal or current signal calculated using Eq. (10) [26].

$$MAF_{out,vd} = \frac{n}{T} \int_{t-\frac{T}{n}}^t V_d dt \quad (5)$$

Where V_d is the d value of the source voltage signal and i_d is the d value of the source current signal.

METHODS

A. Circuit Design of S-APF

In a balanced power, a nonlinear load causes the important amount of harmonics in voltages. Voltage harmonics causes the flow of nonlinear currents in transformers. Transformer windings can be burned at values below standard loads. The S-APF eliminates the voltage sag/swell, voltage unbalances and source voltage harmonics caused by nonlinear loads [18].

The S-APF consists of series source to the power system to the grid using a common DC bus line and IGBT inverters which can operate in voltage controlled mode. Fig. 4 shows a block diagram of a S-APF.

The series active power filter is used to add compensation voltage equally but inversely to the harmonic component of the nonlinear voltages in the phase, in the three-phase system. These voltages are called compensation voltages since they are used to protect the harmonics from nonlinear phase voltages. S-APF produces compensation voltages using phase voltages and currents [19].

B. Proposed Control Algorithm

In the proposed control algorithm, the MAF is used instead of classical LPF to improve the dynamic filtering response and THD and the SV-PWM is used instead of the sinusoidal-PWM to improve the switching performance. Fig. 5 shows the block schema of SRF-based proposed control algorithm.

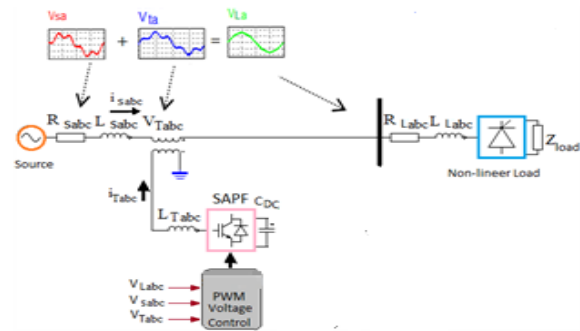


Fig. 4 The topology of a three phase S-APF

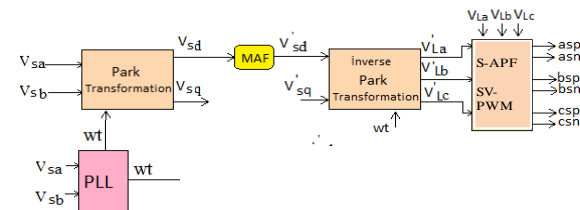


Fig. 5 The block schema of SRF based proposed control algorithm

The ab source voltages (V_{sab}) and abc load voltages (V_{Labc}) are realized by taking five different measurement values in the proposed control algorithm. The PLL circuit is used to obtain the wt transformation angle shown in Fig. 6.

The phase c of the voltage used as the input voltage of the PLL block diagram is calculated by using Eq. (6).

$$V_{sc} = -V_{sa} - V_{sb} \quad (6)$$

The d-q values V_{dpll} and V_{qpll} of the source abc voltages are obtained by using Eq. (7).

$$v_{dpll} = \frac{2}{3} \left(\cos(wt)v_{sa} + \cos\left(wt - \frac{2\pi}{3}\right)v_{sb} + \cos\left(wt + \frac{2\pi}{3}\right)v_{sc} \right)$$

$$v_{qpu} = \frac{2}{3} \left(-\sin(\omega t)v_{sa} - \sin\left(\omega t - \frac{2\pi}{3}\right)v_{sb} - \sin\left(\omega t + \frac{2\pi}{3}\right)v_{sc} \right)$$

$$v_0 = \frac{2}{3} \left(\frac{1}{2}v_{sa} + \frac{1}{2}v_{sb} + \frac{1}{2}v_{sc} \right) \quad (7)$$

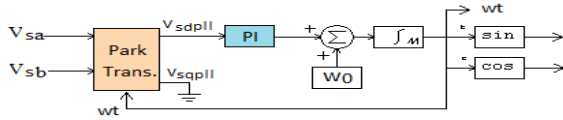


Fig. 6 PLL control circuit

The V_{dp11} is passed through the PI controller and the references are added to the fundamental angular frequency ($2\pi f$). Finally, a ωt is obtained by the integration of this calculation [15].

In the S-APF, the d-q values of the source abc voltages are obtained by using the Eq. (8) with the transformation of dq0. The PLL circuit is used to obtain the ωt transformation angle. The obtained d value is passed from the MAF.

$$v_{sd} = \frac{2}{3} \left(\cos(\omega t)v_{sa} + \cos\left(\omega t - \frac{2\pi}{3}\right)v_{sb} + \cos\left(\omega t + \frac{2\pi}{3}\right)v_{sc} \right)$$

$$v_{sq} = \frac{2}{3} \left(\sin(\omega t)v_{sa} + \sin\left(\omega t - \frac{2\pi}{3}\right)v_{sb} + \sin\left(\omega t + \frac{2\pi}{3}\right)v_{sc} \right)$$

$$v_{s0} = \frac{2}{3} \left(\frac{1}{2}v_{sa} + \frac{1}{2}v_{sb} + \frac{1}{2}v_{sc} \right) \quad (8)$$

The reference load voltages $v'_{La}, v'_{Lb}, v'_{Lc}$ are calculated from the obtained $V'_{sd}, V'_{sq} = 0$ and $V'_{s0} = 0$ using the inverse park transform in (9).

$$V'_{La} = \cos(\omega t)V'_{sd} + \sin(\omega t)V'_{sq} + V'_{s0}$$

$$V'_{Lb} = \cos\left(\omega t - \frac{2\pi}{3}\right)V'_{sd} + \sin\left(\omega t - \frac{2\pi}{3}\right)V'_{sq} + V'_{s0}$$

$$V'_{Lc} = \cos\left(\omega t + \frac{2\pi}{3}\right)V'_{sd} + \sin\left(\omega t + \frac{2\pi}{3}\right)V'_{sq} + V'_{s0} \quad (9)$$

The obtained $V'_{La}, V'_{Lb}, V'_{Lc}$ are compared with the sensed V_{La}, V_{Lb}, V_{Lc} and the switching signals for series inverter are obtained using SV-PWM technique.

RESULTS AND DISCUSSION

Simulation studies to verify the performance of the proposed controller have been tested with the PSIM software program. The values using in the simulation model are shown in Table 1.

The steady state and dynamic performances of three phase S-APF system are analyzed by simulating the system in PSIM software. As a load, a nonlinear load with three-phase thyristor is used. The time setting used for the simulation is 0.5e-6s.

TABLE I: simulation values

Source	
V_{sabc}	190Vrms
f	50Hz
R_{sabc}	10m Ω
L_{sabc}	0.1mH
Load	
R_{sabc}	0.25 Ω
L_{sabc}	1.47mH
R_L	30 Ω
L_L	11.53mH
S-APF	
R_{Fabc}	0.65m Ω
L_{Fabc}	3mH
f_{PWM}	18kHz
C_1	2350 μ F
V_{dc}	400V

Fig. 7 shows the PSIM simulation model of the three-phase S-PWM. S-APF is attributed in series with the system to eliminate voltage problems in the grid and generate sinusoidal voltage. The obtained reference abc voltages are compared with the sensed source abc voltages. The S-APF is operated as a closed-loop controller by generating the reference load voltage currents to correct events that cause power quality problems related to nonlinear loads by continuously reading the source or load voltage according to the control algorithm used.

Fig. 8 shows the effect of S-APF after applying the proposed controller with 5th harmonic component to source voltage and RL load. As given in Fig. 8, the source voltage harmonic is reduced from 15.848% to 0.13. Fig. 9 shows the effect of S-APF after applying the proposed controller with 5th and 7th harmonic component to source voltage and RL load. As given in Fig. 9, the source voltage harmonic is reduced from 19.09% to 0.15%. In the figure 8 and figure 9, the total harmonic distortion ratio is below the harmonic limit applied in IEEE 519-1992 standards.

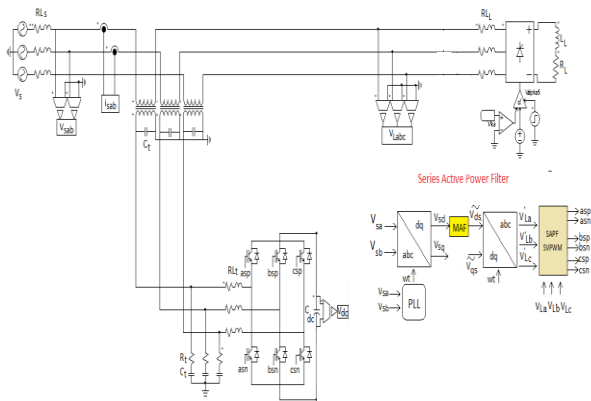


Fig. 7 The simulation block S-APF system

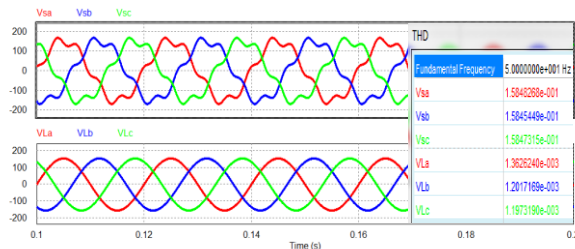


Fig. 8 The V_{sa} , V_{sb} and V_{sc} signals with 5th harmonic component and the V_{La} , V_{Lb} , V_{Lc} signals obtained after applying the proposed control algorithm

Fig. 10 shows the FFT values of load and source voltage THD levels after the proposed SRF based control algorithm. In the obtained results, the source voltage signal consist of main frequency component, 5th harmonic component, 7th harmonic component and the load voltage signal consist of main frequency component.

The simulation results for reactive power compensation are shown in Fig. 11. The power factor values before and after applying the proposed controller are shown in Fig. 11. The power factor between the load voltage and the source current is measured as 0.9999 after the proposed controller is applied to the S-APF system. The proposed control algorithm has the ability to improve the power factor. The study of the proposed controller is tested when the unbalanced nonlinear load is connected. Fig. 12 shows the abc source voltages and the abc load voltages signals before and after applying the proposed controller for three UPQC system. The unbalanced of the source and load voltages are 20%. Fig. 12 b illustrates the abc load voltages without

unbalance and perfectly maintained with proposed controller.

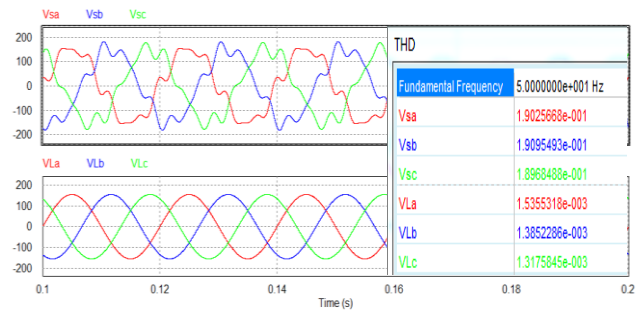


Fig. 9 The V_{sa} , V_{sb} and V_{sc} signals with 5th and 7th harmonic component and the V_{La} , V_{Lb} , V_{Lc} signals after applying the proposed control algorithm

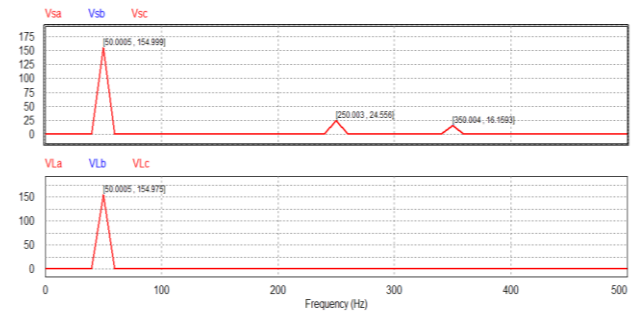


Fig. 10 The FFT values of source and load voltage signals before and after the proposed control algorithm

The study of the proposed control algorithm is tested under transient response and steady state. Fig. 13 shows the transient response of the proposed controller in case of an S-APF system is applied at $t=0.15$ ms. The steady-state response of the proposed control algorithm is shown in Fig. 14.

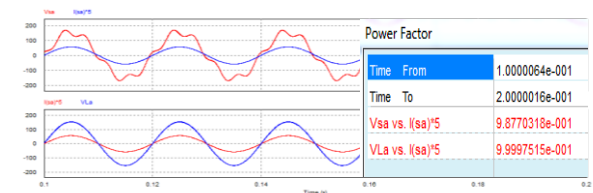


Fig. 11 The load voltage and the source current signals for power factor

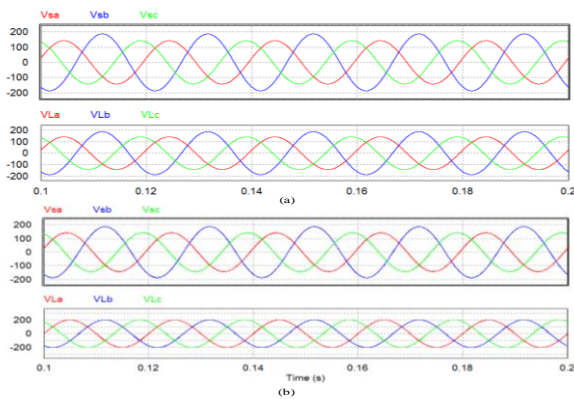


Fig. 12 The V_{sa} , V_{sb} , V_{sc} signals and the V_{La} , V_{Lb} , V_{Lc} signals obtained a) before applying the proposed controller b) after applying the proposed controller with unbalanced nonlinear load

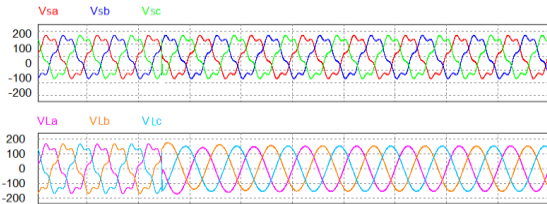


Fig. 13 The simulation results for transient operation of S-APF system for proposed controller a) V_{sa} , V_{sb} and V_{sc} signals, b) V_{La} , V_{Lb} , V_{Lc} signals,

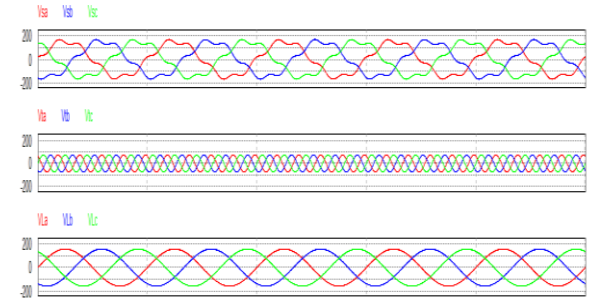


Fig. 14 The simulation results for steady state operation of S-APF system for proposed controller a) V_{sa} , V_{sb} and V_{sc} signals, b) transformer V_{ta} , V_{tb} and V_{tc} signals, c) V_{La} , V_{Lb} , V_{Lc} signals

TABLE II: FONT SIZES FOR PAPERS

Control algorithms	Without filter THD (%)	With filter THD (%)
	Load voltage	Load voltage
PQ algorithm	15.86%	1.94%
Conventional SRF algorithm	15.86%	1.08%
Proposed SRF based control algorithm with MAF and SV-PWM	19.09%	0.15%

In Table 2, the proposed controller and the other control algorithms used in literature for S-APF are compared. In the simulation studies, when the conventional SRF control algorithm is applied to the S-APF, the THD value of the voltage is decreased from 15.86% to 1.94%. When the SRF-based proposed controller is applied to the S-APF, the THD value of the voltage is decreased to 0.15%.

CONCLUSIONS

A new SRF-based control algorithm which applies a moving average filter and SV-PWM to obtain the reference voltage signals for serial active power filter is presented and tested in PSIM. In the proposed control algorithm, MAF filter and space vector pulse width the modulation technique are used to produce the switching signals of the active switches used in serial filter to the reduced THD and

improved PF. In the proposed control algorithm, five measurement values are taken from the power system by using abc source voltage, abc load voltage. The number of measurements is reduced according to the conventional SRF method. It can be observed that the proposed control algorithm gives the lowest THD value according to other algorithms used in literature as shown in Table II. According to Table II, it is seen that the proposed control algorithm is more successful in eliminating the harmonic of the load voltage by improving power factor and by compensating the reactive power.

REFERENCES

- [1]. J. Ye, H. B. Gooi and F. Wu, "Optimization of the Size of UPQC System Based on Data Driven Control Design," *IEEE Transactions on Smart Grid*, vol. 9, pp. 2999-3008, 2016.

- [2]. M. Brenna, R. Faranda and E. Tironi, "A new proposal for power quality and custom power improvement: OPEN UPQC," *IEEE Transactions on Power Delivery*, vol. 24, pp. 2107-2116, 2009.
- [3]. Xiu and Y. Liu, "Hysteresis Response Neural Network and Its Applications," *ISECS International Colloquium on Computing, Communication, Control, and Management*, vol. 1, pp. 361-364, 2009.
- [4]. L. Feng and Y. Wang, "Modeling and Resonance Control of Modular Three Level Shunt Active Power Filter," *IEEE Transactions on Industrial Electronics*, vol. 64, pp. 7478-7486, 2017.
- [5]. D.M. Soomro, M.A. Omran and S.K. Alswed, "Design of A Shunt Active Power Filter to Mitigate the Harmonics Caused by Nonlinear Loads," *ARNP Journal of Engineering and Applied Sciences*, vol. 10, pp. 8774-8782, 2015.
- [6]. C.H. Silva, R.R. Pereira and B.E.L. Silva, "Lambert T.G., Bose B.K. 2008. Improving the Dynamic Response of Shunt Active Power Filter using Modified Synchronous Reference Frame PLL," in *Proc. 34th Annual Conference of IEEE Industrial Electronics*, 2008, p.790-795.
- [7]. M. I. M. Montero, E. R. Cadaval and Gonzalez F. B., "Comparison of control strategies for shunt active power filters in three-phase four-wire systems," *IEEE Trans. Power Electron.*, vol. 22, pp. 229-236, 2007.
- [8]. M. Danbunrungtrakul, T. Saengsuwan and P. Srithorn, "Evaluation of DVR Capability Enhancement Zero Active Power Tracking Technique," *IEEE Access*, vol. 5, pp. 10285-10295, 2017.
- [9]. M.M.R. Pereira, M.M.C. Ferreira and M.F. Barbosa, "Comparative Study of STATCOM and SVC Performance on Dynamic Voltage Collapse of an Electric Power System with Wind Generation," *IEEE Latin America Transactions*, vol. 2, pp. 138-145, 2014.
- [10]. M. Kesler and E. Ozdemir, "Synchronous-reference-frame-based control method for UPQC under unbalanced and distorted load conditions," *IEEE Transactions on Industrial Electronics*, vol. 5, pp. 3967-3975, 2011.
- [11]. S.J. Isac, L. Balakumar, and F. Kavin, "Power Quality Improvement by Unified Power Quality Conditioner Based on CSC Topology Using Synchronous Reference Frame Theory," *Journal of Scientific Research*, vol. 24, pp.1982-1988,2016.
- [12]. N. Zaveri and A. Chudasama, "Control Strategies for Harmonic Mitigation and Power Factor Correction Using Shunt Active Filter under Various Source Voltage conditions," *International Journal for Electrical Power and Energy Systems*, vol. 42, pp. 661-671, 2012.
- [13]. Z. Wang,, Q. Wang,, W. Yao and J. Liu, "A series active power filter adopting hybrid control approach," *IEEE Transactions on Power Electronics*, vol. 16, pp. 301-310, 2001.
- [14]. L. Moran, I. Pastorini, J. Dixon and R. Wallace, "Series active power filter compensates current harmonics and voltage unbalance simultaneously," *IEE Proc., Gener. Transm. Distrib.*, vol. 147, pp. 31-36, 2000.
- [15]. Y. S. Kim, J. S. Kim and S. H. Ko, "Three-phase three-wire series active power filter, which compensates for harmonics and reactive power," *IEE Proceedings-Electric Power Applications*, vol. 151, pp. 276-282, 2004.
- [16]. S. Bhattacharya, D.M. Divan and B. Banerjee, "Synchronous frame harmonic isolator using active series filter," in *Proc. EPE '91, European Conference on Power Electronics and Application*, 1991, p. 3-030-3-035.
- [17]. S. Srianthumrong, H. Fujita and H. Akagi, "Stability analysis of a series active filter integrated with a double-series diode rectifier," *IEEE Trans. Power Electron.*, vol. 17, pp. 117-124, 2002,
- [18]. A.J. Viji and A.A.T. Victoire, "Enhanced PLL based SRF control method for UPQC with fault protection under unbalanced load conditions," *International Journal of Electrical Power and Energy Systems*, vol. 58, pp. 319-328, 2014.
- [19]. N.I. Raju, M.S. Islam and A. A. Uddin, "Sinusoidal PWM Signal Generation Technique for Three Phase Voltage Source Inverter with Analog Circuit & Simulation of PWM Inverter for Standalone Load Micro System," *International Journal of Renewable Energy Research*, vol. 3, pp. 647-658, 2013.
- [20]. Sahoo K.S. and Bhattacharya T., "Phase Shifted Carrier-Based Synchronized Sinusoidal

- PWM Techniques for a Cascaded H-Bridge Multilevel Inverter," *IEEE Transactions on Power Electronics*, vol. 33, pp. 513-524, 2018.
- [21]. R. Patel and A. K. Panda, "Real time implementation of PI and fuzzy logic controller based 3-phase 4-wire interleaved buck active power filter for mitigation of harmonics with id-iq control strategy, *International Journal of Electrical Power and Energy Systems*, vol. 59, pp. 66–78, 2014.
- [22]. J. W. Kelly, E. G. Strangas and J. M. Miller, "Multiphase space vector pulse width modulation," *IEEE Transactions on Energy Conversion*, vol. 18, pp. 259-264, 2003.
- [23]. Y. Lu, G. Xiao, X. Wang, F. Blaabjerg and D. Lu, "Control strategy for single-phase transformerless three-leg unified power quality conditioner based on space vector modulation," *IEEE Trans. Power Electron*, vol. 31, pp. 2840-2849, 2016.
- [24]. M. Shankar, S. Monisha, H. Shesna, T. Vignesh, N. Sikkandar, S. Sundaramoorthi and S. Venkatesh, "Implementation of space vector pulse width modulation technique with genetic algorithm to optimize unified power quality conditioner," *Am. J. Appl. Sci.*, vol.11, pp. 152-159, 2014.
- [25]. S. A. O. Silva and F. A. Negrao, "Single phase to three phase unified power quality conditioner applied in single wire earth return electric power distribution grids," *IEEE Transactions on Power Electronics*, vol. 33, pp. 3950-3960, 2018.
- [26]. S. Devassy and B. Singh, "Design and performance analysis of three-phase solar PV integrated UPQC," *IEEE T. Industry Applications*, vol. 54, pp. 73-81, 2017.

AUTHOR PHOTOS AND BIOGRAPHY

Yasemin Onal was born in Giresun, Turkey. She received her electrical teacher degree from Kocaeli University in 2000 and her Ph.D. from the Electrical and Electronics Engineering Department, Anadolu University, Eskisehir, Turkey, in 2011. She is currently an assistant professor in the Electrical and Electronics Engineering Department, Bilecik Seyh Edebali University, Bilecik, Turkey. Her research areas include power electronic, power quality, active power filter and digital signal processing.